ORIGINAL PAPER

Phosphoglycerate Mutase 1 Promotes Cell Proliferation and Neuroblast Differentiation in the Dentate Gyrus by Facilitating the Phosphorylation of cAMP Response Element-Binding Protein

Hyo Young Jung[1] · Hyun Jung Kwon[2] · Woosuk Kim[1] · Sung Min Nam[3] · Jong Whi Kim[1] · Kyu Ri Hahn[1] · Dae Young Yoo[4] · Moo-Ho Won[5] · Yeo Sung Yoon[1] · Dae Won Kim[2] · In Koo Hwang[1]

Abstract

In a previous study, we observed a significant increase in phosphoglycerate mutase 1 (PGAM1) levels after pyridoxine treatment. In the present study, we investigated the effects of PGAM1 on novel object recognition, cell proliferation, and neuroblast differentiation in the dentate gyrus. We generated a Tat-PGAM1 fusion protein to cross the blood–brain barrier and neuronal plasma membrane. We administered the Tat peptide, control-PGAM1, or Tat-PGAM1 fusion protein to 8-week-old mice once a day for 3 weeks and tested novel object recognition memory. The mice were then euthanized to conduct western blot analysis for polyhistidine expression and immunohistochemical analysis for Ki67, doublecortin, and phosphorylated cAMP response element-binding protein. Mice treated with Tat peptide showed similar exploration times for familiar and new objects and the discrimination index was significantly lower in this group than in the control group. Tat-PGAM1 moderately increased the exploration time of new objects when compared to familiar objects, while the discrimination index was significantly higher in the Tat-PGAM1-treated group, but not in the control-PGAM1-treated group, when compared with the control group. Higher PGAM1 protein expression was observed in the hippocampus of Tat-PGAM1-treated mice when compared with the hippocampi of control, Tat peptide-, and control-PGAM1-treated mice, using western blot analysis. In addition, the numbers of proliferating cells and differentiated neuroblasts were significantly lower in the Tat peptide-treated group than in the control group. In contrast, the numbers of proliferating cells and differentiated neuroblasts in the dentate gyrus were higher in the Tat-PGAM1-treated group than in the control group. Administration of Tat-PGAM1 significantly facilitated the phosphorylation of cAMP response element-binding protein in the dentate gyrus. Administration of control-PGAM1 did not show any significant effects on novel object recognition, cell proliferation, and neuroblast differentiation in the dentate gyrus. These results suggest that PGAM1 plays a role in cell proliferation and neuroblast differentiation in the dentate gyrus via the phosphorylation of cAMP response element-binding protein in the hippocampus.

Keywords Phosphoglycerate mutase 1 · Dentate gyrus · Novel object recognition · Neurogenesis

Hyo Young Jung and Hyun Jung Kwon are equally contributed to this article.

✉ Dae Won Kim
kimdw@gwnu.ac.kr

✉ In Koo Hwang
vetmed2@snu.ac.kr

[1] Department of Anatomy and Cell Biology, College of Veterinary Medicine, and Research Institute for Veterinary Science, Seoul National University, Seoul 08826, South Korea

[2] Department of Biochemistry and Molecular Biology, Research Institute of Oral Sciences, College of Dentistry, Gangneung-Wonju National University, Gangneung 25457, South Korea

[3] Department of Anatomy, College of Veterinary Medicine, Konkuk University, Seoul 05030, South Korea

[4] Department of Anatomy, College of Medicine, Soonchunhyang University, Cheonan, Chungcheongnam 31151, South Korea

[5] Department of Neurobiology, School of Medicine, Kangwon National University, Chuncheon 24341, South Korea

Introduction

Neural stem cells reside in the adult mammalian brain, including humans, and contribute to brain plasticity throughout life [1, 2]. Two major neurogenic areas have been reported in the adult mammalian brain, one of which is the subgranular zone within the dentate gyrus of the hippocampus. Newly generated neurons may participate in the formation of spatial memory [3] and adult neurogenesis-deficient animals show impairment in spatial learning [4]. In the dentate gyrus, progenitors expand and may differentiate into neuroblasts. Then, these cells migrate into the granule cell layer to become mature neurons [5]. Neural stem cells are known to utilize glycolytic metabolism for maintaining self-renewal and lineage potency and then switch to oxidative metabolism during differentiation, which is needed to support the growing energy demands of specialized progeny [6].

Phosphoglycerate mutase (PGAM, E.C. 5.4.2.1) is an enzyme of the anaerobic glycolysis pathway where it catalyzes the conversion of 3-phosphoglycerate to 2-phosphoglycerate [7]. Several lines of evidence demonstrate that PGAM is increased in various cancer tissues including in the brain [8–14], and high levels of PGAM1 expression indicate a high grade of gliomas [15, 16]. Conversely, knockdown or targeting of PGAM1 attenuates cell proliferation in cancer tissues [17, 18] and inhibits glioma cell proliferation and migration in vitro [15]. PGAM1 is believed to be a novel molecular target for cancer treatment [17, 19]. Endogenous PGAM1 is expressed in the endothelium of capillaries as well as arteries in all regions of the brain including the hippocampus [20]. It has been reported that PGAM1 levels are decreased in the hippocampus in several neurological disorders including phenylketonuria [21], hypoxia [22], and schizophrenia [23, 24]. In addition, knockdown of PGAM1 results in partial reduction in glycolysis and cancer cell motility [25]. In contrast, in a previous study, we demonstrated that pyridoxine significantly increased cell proliferation and neuroblast differentiation in the dentate gyrus [26] and, using a proteomics approach, we also validated that these effects are associated with the up-regulation of PGAM1 in the hippocampus [27]. However, we did not confirm the direct effects of PGAM1 on novel object recognition, cell proliferation, and neuroblast differentiation in the dentate gyrus.

Blood vessels in the central nervous system are continuous, non-fenestrated vessels and consist of astrocytes and specialized endothelial cells that allow them to tightly regulate the movement of molecules, ions, and cells between the blood and the central nervous system [28, 29]. In addition, cells have a lipophilic barrier in the cellular membrane, which makes it difficult to deliver large molecules and also small particles into the cell so that they can perform their biological functions. Transactivator of transcription (Tat) from human immunodeficiency virus (HIV) can pass very efficiently through the cell membranes of cultured mammalian cells [30, 31]. Previous studies have demonstrated that Tat-fusion proteins are able to cross the blood–brain barrier and can be delivered to the intracellular space [32, 33]. In the present study, therefore, we generated a Tat-PGAM1 fusion protein to facilitate the crossing of the blood–brain barrier and elucidated the effects of this protein on novel object recognition memory, cell proliferation, and neuroblast differentiation in the dentate gyrus.

Experimental Procedures

Experimental Animals

Male C57BL/6J mice (7 weeks of age, $n = 40$) were purchased from Jackson Laboratory Co. Ltd (Bar Harbor, ME, USA). Five animals were housed per cage in a conventional area under standard conditions at ambient temperature (22 ± 2 °C) and humidity ($60 \pm 5\%$) on a 12/12 h light/dark cycle with ad libitum access to food and water. Animal handling and care conformed to the guidelines of current international laws and policies (National Institutes of Health Guide for the Care and Use of Laboratory Animals, Publication No. 85-23, 1985, revised 1996) and were approved by the Institutional Animal Care and Use Committee of Seoul National University (SNU-170417-19-1). All experiments were conducted with an effort to minimize the number of animals used and the physiological stress caused by the procedures employed. All experimental procedures were conducted according to ARRIVE guidelines [34].

Construction of Expression Vectors

A cell-permeable Tat expression vector was prepared in the laboratory as previously described [35]. The cDNA sequence of human PGAM1 was amplified by polymerase chain reaction (PCR) using the PGAM1 specific sense primer 5′-CTC GAG ATG GCC GCC TAC A-3′ and the PGAM1 specific anti-sense primer 5′-GGA TCC TCA CTT CTT GGC CTT-3′. PCR products were excised, eluted (Expin Gel; GeneAll Biotechnology Co., Ltd., Seoul, Korea), and ligated into a TA cloning vector (pGEM®-T easy vector; Promega Corporation, Madison, WI, USA) according to the manufacturer's protocol. The purified TA vector containing human PGAM1 cDNA was ligated into the Tat expression vector to produce a Tat-PGAM1 fusion protein. The recombinant expression plasmid consisted of 6His-Tat-PGAM1 in a pET-15 vector. We also constructed 6His-PGAM1 without Tat as a control.

To produce the Tat-PGAM1 and control-PGAM proteins, the plasmid was transformed into *Escherichia coli* BL21 cells. The transformed bacterial cells were grown in 100 mL of lysogeny broth media to a D600 value of 0.5–1.0 and then induced with 0.5 mM isopropyl β-D-1-thiogalactopyranoside at 18 °C for 18 h. Harvested cells were lysed by sonication and purified using a Ni^{2+}-nitrilotriacetic acid Sepharose affinity column (Qiagen, Inc.) and PD-10 column chromatography (GE Healthcare, Chicago, IL, USA). The concentration of purified proteins was estimated using a Bradford assay [36].

Equal amounts of protein were analyzed using 10% sodium dodecyl sulfate polyacrylamide gel electrophoresis (SDS-PAGE). Proteins were then electrotransferred to a polyvinylidene difluoride membrane. The membrane was blocked with tris-buffered saline (25 mM Tris–HCl, 140 mM NaCl, 0.1% Tween 20, pH 7.5) containing 5% non-fat dry milk and subsequently probed using anti-polyhistidine antibodies (1:2000, His-probe, SantaCruz Biotechnology, Santa Cruz, CA, USA). Proteins were identified using chemiluminescent reagents as recommended by the manufacturer (Amersham, Franklin Lakes, NJ, USA).

Administration of Tat-PGAM1

Following a 1-week acclimation to laboratory conditions, mice were divided into 4 groups ($n = 10$ in each group): control, Tat peptide-, control-PGAM1-, and Tat-PGAM1-treated groups. Tat peptide (2 mg/kg), control-PGAM1, and Tat-PGAM1 (10 mg/kg) were intraperitoneally administered to mice at 8 weeks of age, once a day for 3 weeks.

Novel Object Recognition Test

The testing apparatus consisted of an open box (25 cm × 25 cm × 25 cm) made of black acrylic as previously described [27]. The floor was covered with woodchip bedding, which was moved around between trials and testing days to prevent the build-up of odor in certain places. The objects to be discriminated were made of solid metal and could not be displaced by the mice due to their weight. The objects were cleaned with bleach to remove residual odors.

On the 20th day of treatment with control, Tat peptide, control-PGAM1-, or Tat-PGAM1, 1 h after treatment, mice from each group ($n = 10$ per group) were allowed to explore the apparatus for 2 min. On the testing day (21st day of treatment), two 2-min trials were performed 1 h after the last treatment. In the sample trial, two identical objects were placed in two opposite corners of the apparatus. Mice were placed in the apparatus and left to explore these two identical objects. After the sample trial, mice were placed back in their home cage for an inter-trial interval of 1 h; subsequently, a choice trial was performed. In the choice trial, a new object replaced one of the objects that were present in the sample trial. The mice were exposed again to two different objects: the familiar and new objects. Exploration was defined as directing the nose toward the object at a distance of no more than 2 cm and/or touching the object with the nose. From this measure, a series of variables were then calculated: the total time spent in exploring the two identical objects in the sample trial and the time spent exploring the two different objects in the choice trial.

The distinction between familiar and new objects in the choice trial was determined by comparing the time spent exploring the familiar object with the time spent exploring the new one. The discrimination index represents the difference in exploration time expressed as a proportion of the total time spent exploring the two objects in the choice trial.

Confirmation of Tat-PGAM1 Delivery into Hippocampus

Following the novel object recognition test, animals in the control, Tat peptide-, control-PGAM-, and Tat-PGAM1-treated groups ($n = 5$ in each group) were sacrificed. Brain tissue was analyzed by western blotting as previously described [27]. Following sacrifice and the removal of tissues, the tissues were cut into 500-μm-thick sections on a vibratome (Leica Microsystems GmbH) and the hippocampus was dissected using a surgical blade. Hippocampal tissues were homogenized in 50 mM phosphate-buffered saline (PBS, pH 7.4) containing 0.1 mM ethylene glycol-bis(β-aminoethyl ether)-*N,N,N′,N′*-tetraacetic acid (pH 8.0), 0.2% Nonidet P-40, 10 mM ethylenediaminetetraacetic acid (pH 8.0), 15 mM sodium pyrophosphate, 100 mM β-glycerophosphate, 50 mM sodium fluoride, 150 mM sodium chloride, 2 mM sodium orthovanadate, 1 mM phenylmethylsulfonyl fluoride and 1 mM dithiothreitol (DTT). Following centrifugation for 5 min at 16,000×*g* at 4 °C, the protein concentration in the supernatants was determined using a Micro BCA protein assay kit with bovine serum albumin as the standard (Pierce; Thermo Fisher Scientific, Inc., Waltham, MA, USA). Aliquots containing 20 μg of total protein were boiled in loading buffer containing 150 mM Tris (pH 6.8), 3 mM DTT, 6% SDS, 0.3% bromophenol blue, and 30% glycerol. Each aliquot was subsequently loaded onto a polyacrylamide gel. Following electrophoresis, the proteins in the gel were transferred to a nitrocellulose membrane (Pall Life Sciences, Port Washington, NY, USA). To reduce background staining, the membrane was incubated with 5% non-fat dry milk in PBS containing 0.1% Tween-20 for 45 min at 25 °C, which was followed by incubation with rabbit anti-polyhistidine primary antibody (1:2000, His-probe, SantaCruz Biotechnology), peroxidase-conjugated goat anti-rabbit IgG (1:5000, SantaCruz Biotechnology), and

an ECL chemiluminescent reagent (Pierce; Thermo Fisher Scientific, Inc.).

Tissue Processing

Following the novel object recognition test, animals ($n = 5$ in each group) were anesthetized with 1 g/kg of urethane (Sigma-Aldrich, St. Louis, MO, USA) and perfused transcardially with 0.1 M PBS (pH 7.4) followed by 4% paraformaldehyde in 0.1 M PBS (pH 7.4) as previously described [27]. The brains were dissected and post-fixed for 12 h in the same fixative. The tissue was cryoprotected by overnight saturation with 30% sucrose. Serial brain sections were cut coronally at a thickness of 30 μm using a cryostat (Leica, Wetzlar, Germany) and collected in 6-well plates containing PBS for further processing.

Immunohistochemistry

All sections were processed under the same conditions to ensure that the immunohistochemical data were comparable. Tissue sections, at 90 μm intervals, were selected from an area between 1.82 and 2.30 mm posterior to the bregma, as defined by a mouse atlas [37]. The sections were sequentially treated with 0.3% H_2O_2 in PBS for 30 min and 10% normal goat serum in 0.05 M PBS for 30 min at 25 °C. Sections first underwent overnight incubation with rabbit anti-Ki67 antibody (1:1000; Abcam), rabbit anti-doublecortin (DCX) antibody (1:5000; Abcam) or rabbit anti-phosphorylated cAMP response element-binding protein at Ser133 (pCREB; 1:400; Cell Signaling Technology, Inc., Beverly, MA, USA) at 25 °C. Thereafter, the sections were treated with biotinylated goat anti-rabbit IgG and a streptavidin-peroxidase complex (1:200; Vector, Burlingame, CA, USA) for 2 h at 25 °C. Sections were visualized by reaction with 3,3′-diaminobenzidine tetrachloride (Sigma) in 0.1 M Tris–HCl buffer (pH 7.2) and mounted on gelatin-coated slides. Sections were dehydrated and mounted with Canada balsam (Kanto Chemical, Tokyo, Japan).

Data Analysis

Analysis of the hippocampal dentate gyrus for DCX was performed using an image analysis system and ImageJ software v. 1.50 (National Institutes of Health, Bethesda, MD, USA). Data analysis was carried out under the same conditions by two observers in blinded conditions for each experiment, to ensure objectivity as described in a previous study [27]. Digital images of the whole dentate gyrus were captured using a BX51 light microscope (Olympus, Tokyo, Japan) equipped with a digital camera (DP72, Olympus) connected to a computer. Images were calibrated into an array of 512×512 pixels corresponding to a tissue area

of 1200 μm × 900 μm (100× primary magnification). Each pixel resolution had 256 Gy levels and the intensity of DCX immunoreactivity was evaluated by relative optical density (ROD), which was obtained after transformation of the mean gray level using the following formula: ROD = log(256/mean gray level). The ROD of background staining was determined in unlabeled portions of the sections using Photoshop CC 2018 software (Adobe Systems Inc., San Jose, CA, USA) and this value was subtracted to correct for nonspecific staining using ImageJ v. 1.50 software. Data are expressed as a percentage of the control group (which was set at 100%).

The Ki67- and pCREB-immunoreactive nuclei in the whole dentate gyrus were counted using an analysis system equipped with a computer-based CCD camera (OPTIMAS software version 6.5; CyberMetrics® Corporation, Phoenix, AZ, USA; magnification, 100×) as described in a previous study [27]. The image was converted to a gray-scale image and Ki67- and pCREB-immunoreactive nuclei were automatically selected according to the intensity of the immunohistochemical staining for Ki67 and pCREB, respectively.

Statistical Analysis

The data were expressed as the mean of the experiments performed for each experimental investigation. In order to determine the changes in cell number and ROD, mean differences among the groups were analyzed statistically by one-way analyses of variance followed by Bonferroni's post-hoc test using GraphPad Prism 5.01 software (GraphPad Software, Inc., La Jolla, CA, USA). The results were considered to be statistically significant if $p < 0.05$.
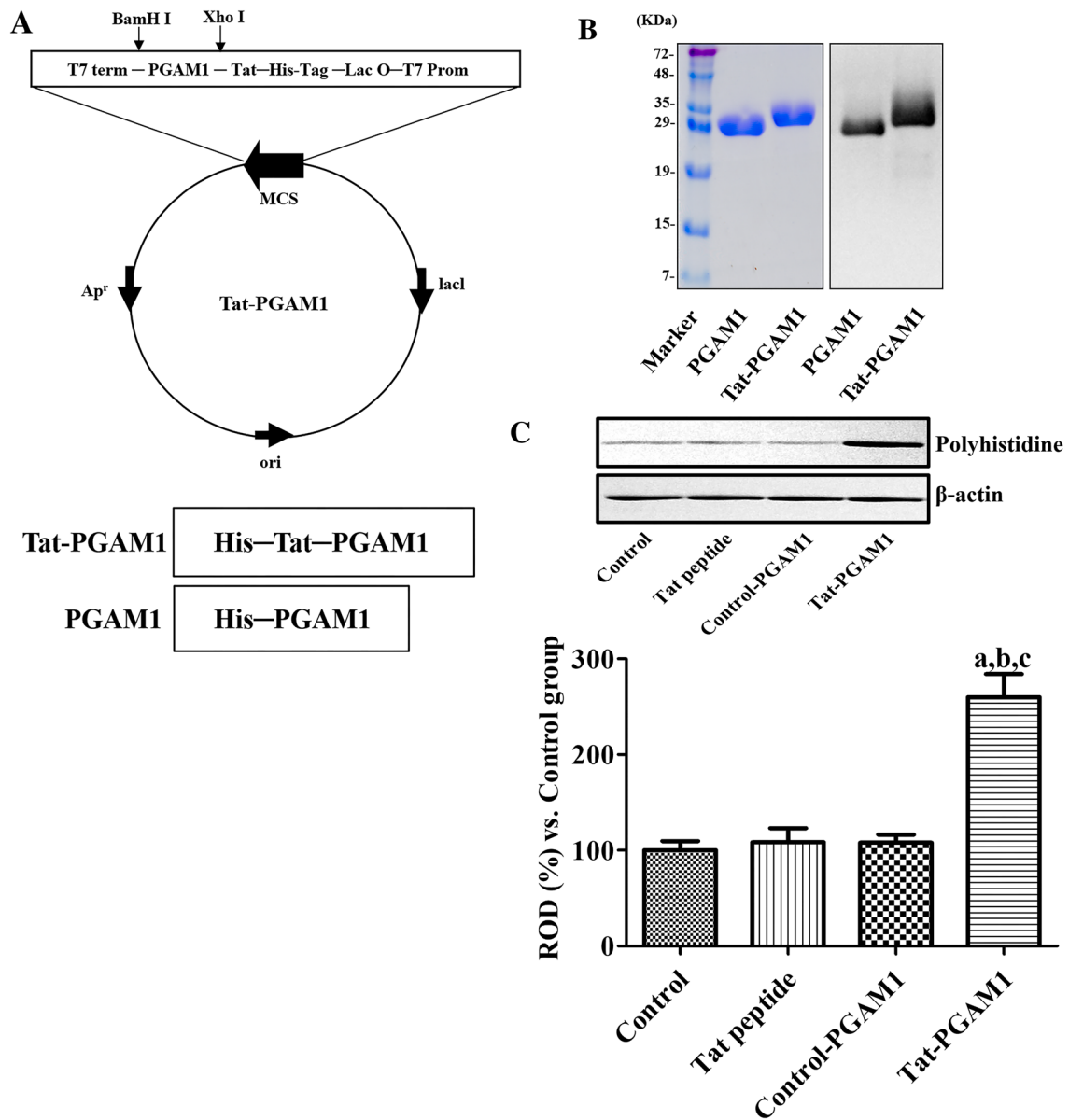
Results

Purification and Identification of Control-PGAM1 and Tat-PGAM1 Fusion Proteins

Human PGAM1 genes were fused to Tat peptide expression vectors to produce the Tat-PGAM1 fusion proteins. Control-PGAM1 protein, without a Tat domain, was manufactured (Fig. 1a). After the overexpression of the vectors, purified control-PGAM1 and Tat-PGAM1 fusion proteins were obtained by Ni^{b+}- → Ni^{2+}-nitrilotriacetic acid Sepharose affinity column and PD-10 column chromatography. Western blot analysis revealed polyhistidine bands for control-PGAM1 and Tat-PGAM1 (Fig. 1b).

Confirmation of Tat-PGAM1 Delivery into the Hippocampus

To confirm the efficient delivery of control-PGAM1 and Tat-PGAM1 fusion proteins into the hippocampus, western blot

Fig. 1 Purification and identification of control-PGAM1 and Tat-PGAM1 fusion proteins and delivery of these proteins into mouse hippocampus. **a** Overview of the control-PGAM1 and Tat-PGAM1 fusion protein. **b** Expression and purification of the control-PGAM1 and Tat-PGAM1 proteins, as assessed by western blot analyses for polyhistidine. **c** Western blot analysis of polyhistidine in hippocampal homogenates of control, Tat peptide-, control-PGAM1-, and Tat-PGAM1-treated groups ($n = 5$ per group; [a]$p < 0.05$, vs. control group; [b]$p < 0.05$, vs. Tat-peptide-treated group; [c]$p < 0.05$, vs. control-PGAM1-treated group)

analysis was conducted. Administration of Tat-PGAM1 significantly increased polyhistidine protein levels in hippocampal homogenates. Administration of Tat peptide or control-PGAM1 resulted in similar polyhistidine protein levels to those in the control group (Fig. 1c).

Effects of Tat-PGAM1 on Novel Object Recognition Memory

Mice spent a similar amount of time exploring the two identical objects in all groups during the training period.
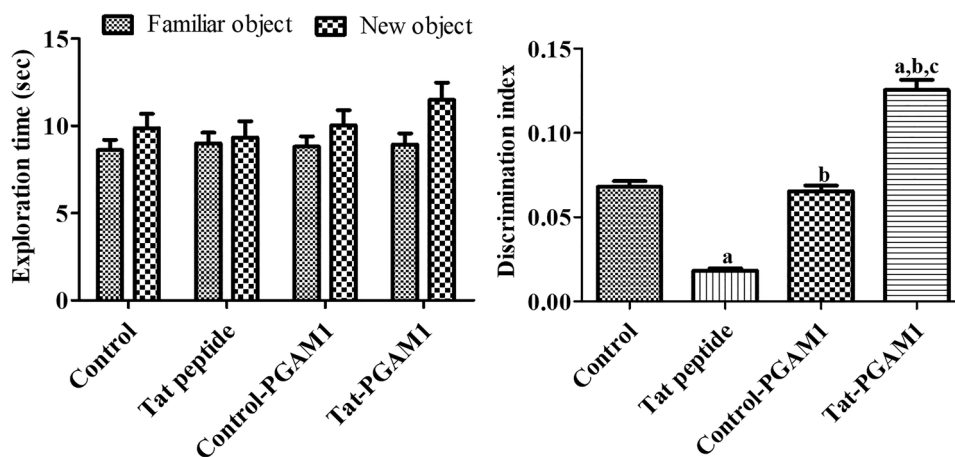
Fig. 2 Exploration time ($n = 10$ per group) and discrimination index ($n = 10$ per group; [a]$p < 0.05$, vs. control group; [b]$p < 0.05$, vs. Tat-peptide-treated group; [c]$p < 0.05$, versus control-PGAM1-treated group) of familiar versus novel objects during testing day of a novel object recognition test in control, Tat peptide-, control-PGAM1-, and Tat-PGAM1-treated mice. Data of the exploration time for each object (same object, where one object was replaced by a new one on the testing day) are presented as a percentage of total exploration time. All data are shown as % exploration time $\pm$ SEM

However, mice in all groups spent more time exploring the new object than the familiar one during the testing period. Mice in the Tat peptide-treated group spent similar time exploring the new and familiar objects, while the Tat-PGAM1-treated group spent more time exploring the new object than the familiar one. However, no statistically significant difference was detected between the control and Tat peptide-treated groups or between the control and Tat-PGAM1-treated groups. It is notable that the discrimination index was significantly lower in the Tat peptide-treated group and higher in the Tat-PGAM1-treated group than in the control or control-PGAM1-treated groups (Fig. 2).

Effects of Tat-PGAM1 on Cell Proliferation in the Dentate Gyrus

In the control group, Ki67-positive proliferating cells were mainly observed in the subgranular zone of the dentate gyrus and the mean number of Ki67-positive nuclei was 12.32 (Fig. 3a, e). In the Tat peptide-treated group, few Ki67-positive proliferating cells were found in the dentate gyrus and the number of Ki67-positive nuclei was lower (by 53.41%) than that in the control group (Fig. 3b, e). In the control-PGAM1-treated group, Ki67-positive proliferating cells were also mainly observed in the dentate gyrus and the number of Ki67-positive nuclei was 11.06 (Fig. 3c, e). In the Tat-PGAM1-treated group, Ki67-positive proliferating cells were observed in the dentate gyrus and the number of Ki67-positive nuclei was significantly higher (by 235.9%) than that in the control group (Fig. 3d, e).
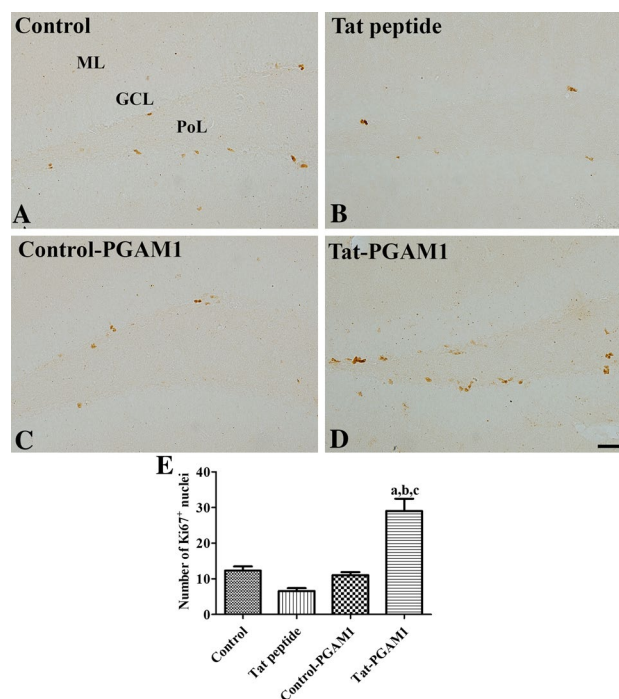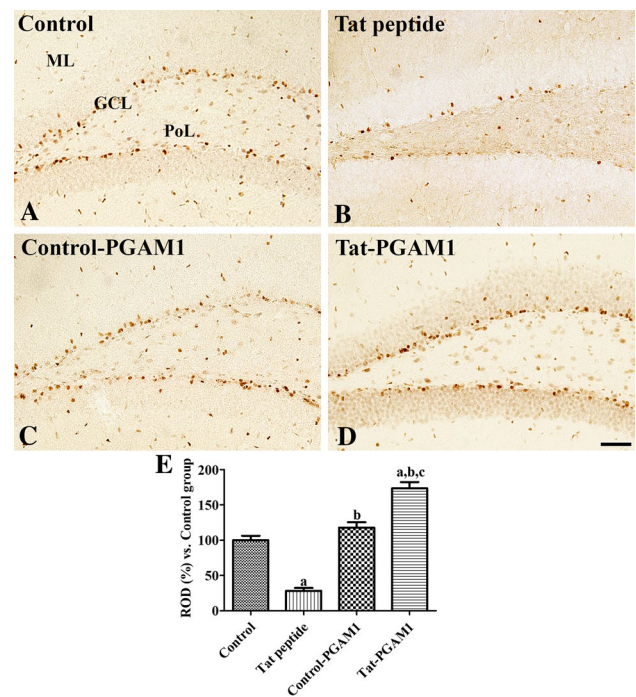

Fig. 3 Immunohistochemistry for Ki67 in the dentate gyrus of **a** control, **b** Tat peptide-, **c** control-PGAM1- and **d** Tat-PGAM1-treated mice. Ki67-positive nuclei are mainly observed in the subgranular zone of the dentate gyrus. Note that Ki67-positive nuclei are few in Tat peptide-treated mice and are most abundant in the dentate gyrus of Tat-PGAM1-treated mice. *GCL* granule cell layer, *ML* molecular layer, *PL* polymorphic layer. Scale bar = 50 μm. **e** The number of Ki67-positive nuclei in the dentate gyrus per section for each group are also shown ($n = 5$ per group; [a]$p < 0.05$, versus control group; [b]$p < 0.05$, versus Tat-peptide-treated group; [c]$p < 0.05$, versus control-PGAM1-treated group). Data are presented as mean $\pm$ SEM
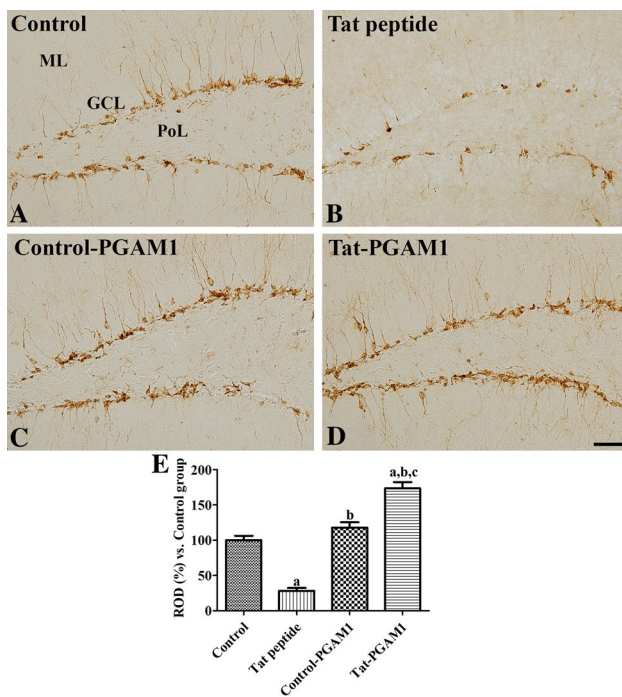
Fig. 4 Immunohistochemistry for DCX in the dentate gyrus of **a** control, **b** Tat peptide-, **c** control-PGAM1- and **d** Tat-PGAM1-treated mice. DCX-immunoreactive neuroblasts have cytoplasm located in the subgranular zone and have dendrites extending into the molecular layer (ML) of the dentate gyrus. DCX-immunoreactive neuroblasts and their dendrites are poorly detected in the dentate gyrus of Tat peptide-treated mice, but are most abundant in the dentate gyrus of Tat-PGAM1-treated mice. *GCL* granule cell layer, *PL* polymorphic layer. Scale bar = 50 μm. **e** The relative optical densities (RODs) expressed as a percentage of the value representing the DCX immunoreactivity in the dentate gyrus of the control group are also shown (*n* = 5 per group; $^{a}p < 0.05$, vs. control group; $^{b}p < 0.05$, vs. Tat-peptide-treated group; $^{c}p < 0.05$, vs. control-PGAM1-treated group). Data are presented as mean ± SEM

Fig. 5 Immunohistochemistry for pCREB in the dentate gyrus of **a** control, **b** Tat peptide-, **c** control-PGAM1- and **d** Tat-PGAM1-treated mice. pCREB-positive nuclei are mainly found in the subgranular zone of the dentate gyrus. Note that pCREB-positive nuclei are few in the dentate gyrus of Tat peptide-treated mice, while pCREB-positive nuclei are strong and most abundant in the dentate gyrus of Tat-PGAM1-treated mice. *GCL* granule cell layer, *ML* molecular layer, *PL* polymorphic layer. Scale bar = 50 μm. **e** The number of pCREB-positive nuclei per section for each group are also shown (*n* = 5 per group; $^{a}p < 0.05$, versus control group; $^{b}p < 0.05$, vs. Tat-peptide-treated group; $^{c}p < 0.05$, vs. control-PGAM1-treated group). Data are presented as mean ± SEM

Effects of Tat-PGAM1 on Neuroblast Differentiation in the Dentate Gyrus

In the control group, DCX-immunoreactive differentiated neuroblasts were detected in the dentate gyrus. In this group, DCX immunoreactivity was found in the cytoplasm and dendrites, which extended into the molecular layer of dentate gyrus (Fig. 4a). In the Tat peptide-treated group, DCX immunoreactive differentiated neuroblasts were few and their dendrites were poorly developed in the dentate gyrus. DCX immunoreactivity was significantly lower, by 28.26%, than that in the control group (Fig. 4b, e). In the control-PGAM1-treated group, DCX-immunoreactive differentiated neuroblasts were observed to have a distribution pattern similar to that in the control group, and DCX immunoreactivity was slightly higher than that in the control group (Fig. 4c, e). The DCX-immunoreactive differentiated neuroblasts were more abundant in the dentate gyrus

in the Tat-PGAM1-treated group than in this region in the control or control-PGAM1-treated group. Further, in the Tat-PGAM1-treated group, DCX immunoreactivity was significantly higher, by 173.56%, than that in the control group (Fig. 4d, e).

Effects of Tat-PGAM1 on the Phosphorylation of CREB in the Dentate Gyrus

In the control group, pCREB-positive nuclei were mainly observed in the subgranular zone of the dentate gyrus and the mean number of pCREB-positive nuclei was 46.70 (Fig. 5a, e). In the Tat peptide-treated group, few pCREB-positive nuclei were found in the dentate gyrus and the number of pCREB-positive nuclei was lower, by 54.05%, than that in the control group (Fig. 5b, e). pCREB positive nuclei were detected in the dentate gyrus both in the control and control-PGAM1-treated groups although the number of pCREB-positive nuclei was slightly higher than

that in the control group (Fig. 5c, e). pCREB-positive nuclei were more abundantly observed in the dentate gyrus in the Tat-PGAM1-treated group than in this region in the control or control-PGAM1-treated group. Moreover, in the Tat-PGAM1-treated group, the number of pCREB-positive nuclei was significantly higher, by 154.7%, than in the control group (Fig. 5d, e).

Discussion

PGAM protein expression is up-regulated in various cancers such as colorectal cancer [8], lung cancer [9], breast carcinoma [10], esophagus squamous cell carcinoma [11], breast cancer, prostate cancer [38], oral squamous cellular carcinoma [12], and glioma [13, 14]. In previous studies, we demonstrated that pyridoxine promoted cell proliferation and neuroblast differentiation in naïve mice [26, 27]. Proteomic approaches demonstrated that pyridoxine increased PGAM1 levels and we confirmed the increase in PGAM1 mRNA levels in the hippocampus after pyridoxine treatment [27]. In the present study, we investigated the role of PGAM1 in cell proliferation and neuroblast differentiation in the mouse dentate gyrus. The data suggest that cancer and hippocampal neurogenesis share a similar microenvironment and metabolic pathways. We examined the effects of PGAM1 on novel object recognition memory, cell proliferation, and neuroblast differentiation in the dentate gyrus.

To facilitate the delivery of PGAM1 into neurons, we generated a Tat-PGAM1 fusion protein attached to a polyhistidine tag and we confirmed the successful expression of Tat-PGAM1 fusion by western blot, probing for polyhistidine in the hippocampus. Administration of Tat-PGAM1 significantly increased the polyhistidine levels in the hippocampus, while control-PGAM1 treatment did not show any significant changes in the levels of polyhistidine. This result indicates that control-PGAM1 was not able to cross the blood–brain barrier or cell membrane, while Tat-PGAM1 fusion protein effectively crossed the blood–brain barrier and cell membrane. Tat-fusion protein can be applied to research on neurological disorders including Alzheimer's disease and cerebral ischemia [39–41].

It has been reported that HIV infection and its associated Tat protein are one of the causative agents in HIV-associated neurocognitive disorders [42, 43]. In addition, Tat peptide has been linked to impaired neurogenesis and cognitive deficits [44, 45]. In the present study, we also observed significant reduction in novel object recognition as well as cell proliferation and neuroblast differentiation in the dentate gyrus. Intrahippocampal administration of Tat protein resulted in behavioral deficits in the Morris water maze and novel object recognition tests in rats [46]. Tat-expressing mouse brains showed significant reduction in the numbers

of neural stem cells and neuroblasts, and integration into mature neurons. In addition, Tat-containing conditioned media showed impairments in proliferation, migration, and differentiation of neural precursor cells through Notch signaling [45]. Administration of Tat-PGAM1 increased the amount of time spent exploring the new object, although statistical significance was not detected. However, the DI was significantly higher in the Tat-PGAM1-treated group than in the control or control-PGAM1-treated groups. This result suggests that administration of Tat-PGAM1 improves novel object recognition memory. To elucidate the effects of Tat-PGAM1 on cell proliferation and neuroblast differentiation in the dentate gyrus, we conducted immunohistochemical staining for Ki67 and DCX, respectively. Administration of Tat-PGAM1, but not control-PGAM1, significantly increased the number of proliferating cells and differentiated neuroblasts in the dentate gyrus. This result suggests that PGAM1 facilitates glycolysis in order to promote cell proliferation and neuroblast differentiation in the dentate gyrus. This result was supported by previous studies that showed that the targeting of PGAM1 with siRNA or its small molecule inhibitor, PGMI-004A, induced cell death by up-regulating the apoptotic pathway and down-regulating the anti-apoptotic pathway [15], attenuated cancer cell proliferation [17, 18], and reduced cell motility [25]. However, a recent study demonstrated that knockdown of PGAM1 only partially reduced glycolysis [25]. Another possibility is that PGAM1 modulates actin filament assembly, cell motility, and cell migration, as shown in cancer cells, through direct interaction with α-smooth muscle actin ACTA2, independent of its metabolic activity [25].

CREB is one of the most important transcription factors mediating neural plasticity in the mammalian brain. Depletion of CREB results in impaired axonal growth and projections [47], while activation of CREB in cortical neurons induces dendritic growth and arborization [48]. In addition, CREB regulates the expression of glucose transporter 3 (GLUT3) and pharmacological inhibition of glycolysis impairs neurite growth [49]. In previous studies, we demonstrated that GLUT3 and glucose metabolism are closely related to hippocampal neurogenesis in the gerbil hippocampus after transient forebrain ischemia [50] as well as postnatal development in mouse hippocampus [51]. Furthermore, we previously demonstrated that administration of pyridoxine significantly increased the number of pCREB-immunoreactive nuclei in the high-fat diet-fed mice [52]. In the present study, we have demonstrated that administration of Tat-PGAM1 significantly increases the phosphorylation of CREB in the dentate gyrus. Collectively, PGAM1 up-regulates the phosphorylation of CREB and facilitates synaptic plasticity, cell proliferation, and neuroblast differentiation, as well as glucose metabolism, in the hippocampus. To confirm the role of PGAM1 on hippocampal neurogenesis

and cognitive functions, a knockout study for PGAM1 needs to be planned as there are currently no knockout mice for *Pgam1*.

In conclusion, the administration of Tat-PGAM1 promotes cell proliferation and neuroblast differentiation in the dentate gyrus by up-regulating the phosphorylation of CREB, and improves novel object recognition ability. Tat-PGAM1 may be useful for the treatment of neurological disorders related to the hippocampus because of its potential to promote regenerative processes.

Author Contributions HYJ, HJK, WK, SMN, JWK, KRH, DYY, MHW, YSY, DWK, and IKH conceived the study. HYJ, HJK, DWK, and IKH designed the study and wrote the manuscript. HYJ, WK, JWK, and KRH conducted the animal experiments and HJK and DWK conducted biochemical experiments. SMN, DYY, MHW, and YSY participated in designing and critical discussing the study. All authors have read and approved the final manuscript.

Data Availability The datasets and supporting materials generated during and/or analyzed during the current study are available from the corresponding author on reasonable request.

Compliance with Ethical Standards

Conflict of interest The authors declare that they have no competing interests.

References

1. Kempermann G, Gage FH (1999) New nerve cells for the adult brain. Sci Am 280:48–53
2. Drew LJ, Fusi S, Hen R (2013) Adult neurogenesis in the mammalian hippocampus: why the dentate gyrus? Learn Mem 20:710–729
3. Kee N, Teixeira CM, Wang AH, Frankland PW (2007) Preferential incorporation of adult-generated granule cells into spatial memory networks in the dentate gyrus. Nat Neurosci 10:355–362
4. Dupret D, Revest JM, Koehl M et al (2008) Spatial relational memory requires hippocampal adult neurogenesis. PLoS ONE 3:e1959
5. Rikani AA, Choudhry Z, Choudhry AM, Zenonos G, Tariq S, Mobassarah NJ (2013) Spatially regulated adult neurogenesis. Ann Neurosci 20:67–70
6. Bond AM, Ming GL, Song H (2015) Adult mammalian neural stem cells and neurogenesis: five decades later. Cell Stem Cell 17:385–395
7. Fothergill-Gilmore LA, Watson HC (1989) The phosphoglycerate mutases. Adv Enzymol Relat Areas Mol Biol 62:227–313
8. Usuba T, Ishibashi Y, Okawa Y, Hirakawa T, Takada K, Ohkawa K (2001) Purification and identification of monoubiquitin-phosphoglycerate mutase B complex from human colorectal cancer tissues. Int J Cancer 94:662–668
9. Li C, Xiao Z, Chen Z et al (2006) Proteome analysis of human lung squamous carcinoma. Proteomics 6:547–558
10. Durany N, Joseph J, Jimenez OM et al (2000) Phosphoglycerate mutase, 2,3-bisphosphoglycerate phosphatase, creatine kinase and enolase activity and isoenzymes in breast carcinoma. Br J Cancer 82:20–27
11. Fang MZ, Liu C, Song Y et al (2004) Over-expression of gastrin-releasing peptide in human esophageal squamous cell carcinomas. Carcinogenesis 25:865–871
12. Turhani D, Krapfenbauer K, Thurnher D, Langen H, Fountoulakis M (2006) Identification of differentially expressed, tumor-associated proteins in oral squamous cell carcinoma by proteomic analysis. Electrophoresis 27:1417–1423
13. Gao H, Yu B, Yan Y et al (2013) Correlation of expression levels of ANXA2, PGAM1, and CALR with glioma grade and prognosis. J Neurosurg 118:846–853
14. Jain R, Kulkarni P, Dhali S, Rapole S, Srivastava S (2015) Quantitative proteomic analysis of global effect of LLL12 on U87 cell's proteome: an insight into the molecular mechanism of LLL12. J Proteomics 113:127–142
15. Xu Z, Gong J, Wang C et al (2016) The diagnostic value and functional roles of phosphoglycerate mutase 1 in glioma. Oncol Rep 36:2236–2244
16. Liu ZG, Ding J, Du C et al (2018) Phosphoglycerate mutase 1 is highly expressed in C6 glioma cells and human astrocytoma. Oncol Lett 15:8935–8940
17. Ren F, Wu H, Lei Y et al (2010) Quantitative proteomics identification of phosphoglycerate mutase 1 as a novel therapeutic target in hepatocellular carcinoma. Mol Cancer 9:81
18. Hitosugi T, Zhou L, Elf S et al (2012) Phosphoglycerate mutase 1 coordinates glycolysis and biosynthesis to promote tumor growth. Cancer Cell 22:585–600
19. Scatena R, Bottoni P, Pontoglio A, Mastrototaro L, Giardina B (2008) Glycolytic enzyme inhibitors in cancer treatment. Expert Opin Investig Drugs 17:1533–1545
20. Jacobowitz DM, Jozwik C, Fukuda T, Pollard HB (2008) Immunohistochemical localization of Phosphoglycerate mutase in capillary endothelium of the brain and periphery. Microvasc Res 76:89–93
21. Imperlini E, Orrù S, Corbo C, Daniele A, Salvatore F (2014) Altered brain protein expression profiles are associated with molecular neurological dysfunction in the PKU mouse model. J Neurochem 129:1002–1012
22. Sharma NK, Sethy NK, Bhargava K (2013) Comparative proteome analysis reveals differential regulation of glycolytic and antioxidant enzymes in cortex and hippocampus exposed to short-term hypobaric hypoxia. J Proteomics 79:277–298
23. Martins-de-Souza D, Alsaif M, Ernst A et al (2012) The application of selective reaction monitoring confirms dysregulation of glycolysis in a preclinical model of schizophrenia. BMC Res Notes 5:146
24. Prabakaran S, Swatton JE, Ryan MM et al (2004) Mitochondrial dysfunction in schizophrenia: evidence for compromised brain metabolism and oxidative stress. Mol Psychiatry 9:684–697
25. Zhang D, Jin N, Sun W et al (2017) Phosphoglycerate mutase 1 promotes cancer cell migration independent of its metabolic activity. Oncogene 36:2900–2909
26. Yoo DY, Kim W, Kim DW et al (2011) Pyridoxine enhances cell proliferation and neuroblast differentiation by upregulating the GABAergic system in the mouse dentate gyrus. Neurochem Res 36:713–721
27. Jung HY, Kim DW, Nam SM et al (2017) Pyridoxine improves hippocampal cognitive function via increases of serotonin turnover and tyrosine hydroxylase, and its association with CB1

cannabinoid receptor-interacting protein and the CB1 cannabinoid receptor pathway. Biochim Biophys Acta 1861:3142–3153

28. Liebner S, Dijkhuizen RM, Reiss Y, Plate KH, Agalliu D, Constantin G (2018) Functional morphology of the blood-brain barrier in health and disease. Acta Neuropathol 135:311–336

29. Daneman R (2012) The blood-brain barrier in health and disease. Ann Neurol 72:648–672

30. Green M, Loewenstein PM (1988) Autonomous functional domains of chemically synthesized human immunodeficiency virus tat trans-activator protein. Cell 55:1179–1188

31. Frankel AD, Pabo CO (1988) Cellular uptake of the tat protein from human immunodeficiency virus. Cell 55:1189–1193

32. Eum WS, Kim DW, Hwang IK et al (2004) In vivo protein transduction: biologically active intact pep-1-superoxide dismutase fusion protein efficiently protects against ischemic insult. Free Radic Biol Med 37:1656–1669

33. Yoo DY, Kim DW, Kwon HJ et al (2017) Chronic administration of SUMO1 has negative effects on novel object recognition memory as well as cell proliferation and neuroblasts differentiation in the mouse dentate gyrus. Mol Med Rep 16:3427–3432

34. Kilkenny C, Browne WJ, Cuthill IC, Emerson M, Altman DG (2010) Improving bioscience research reporting: the ARRIVE guidelines for reporting animal research. PLoS Biol 8:e1000412

35. Kwon HY, Eum WS, Jang HW et al (2000) Transduction of Cu, Zn-superoxide dismutase mediated by an HIV-1Tat protein basic domain into mammalian cells. FEBS Lett 485:163–167

36. Bradford MM (1976) A rapid and sensitive method for the quantitation of microgram quantities of protein utilizing the principle of proteindye binding. Anal Biochem 72:248254

37. Paxinos G, Franklin KBJ (2001) The mouse brain in stereotaxic coordinates. Academic Press, San Diego

38. Cortesi L, Barchetti A, De Matteis E et al (2009) Identification of protein clusters predictive of response to chemotherapy in breast cancer patients. J Proteome Res 8:4916–4933

39. Buccarello L, Borsello T (2017) The Tat-Aβ1-6A2V(D) peptide against AD synaptopathy. Oncotarget 8:10773–10774

40. Tu J, Zhang X, Zhu Y et al (2015) Cell-permeable peptide targeting the Nrf2-Keap1 interaction: a potential novel therapy for global cerebral ischemia. J Neurosci 35:14727–14739

41. Kim SM, Hwang IK, Yoo DY et al (2015) Tat-antioxidant 1 protects against stress-induced hippocampal HT-22 cells death and attenuate ischaemic insult in animal model. J Cell Mol Med 19:1333–1345

42. Gannon P, Khan MZ, Kolson DL (2011) Current understanding of HIV-associated neurocognitive disorders pathogenesis. Curr Opin Neurol 24:275–283

43. Irish BP, Khan ZK, Jain P et al (2009) Molecular mechanisms of neurodegenerative diseases induced by human retroviruses: a review. Am J Infect Dis 5:231–258

44. Ferrell D, Giunta B (2014) The impact of HIV-1 on neurogenesis: implications for HAND. Cell Mol Life Sci 71:4387–4392

45. Fan Y, Gao X, Chen J, Liu Y, He JJ (2016) HIV Tat impairs neurogenesis through functioning as a Notch ligand and activation of Notch signaling pathway. J Neurosci 36:11362–11373

46. Harricharan R, Thaver V, Russell VA, Daniels WM (2015) Tat-induced histopathological alterations mediate hippocampus-associated behavioural impairments in rats. Behav Brain Funct 11:3

47. Lonze BE, Riccio A, Cohen S, Ginty DD (2002) Apoptosis, axonal growth defects, and degeneration of peripheral neurons in mice lacking CREB. Neuron 34:371–385

48. Redmond L, Kashani AH, Ghosh A (2002) Calcium regulation of dendritic growth via CaM kinase IV and CREB-mediated transcription. Neuron 34:999–1010

49. Segarra-Mondejar M, Casellas-Díaz S, Ramiro-Pareta M et al (2018) Synaptic activity-induced glycolysis facilitates membrane lipid provision and neurite outgrowth. EMBO J 37(9):e97368

50. Yoo DY, Lee KY, Park JH et al (2016) Glucose metabolism and neurogenesis in the gerbil hippocampus after transient forebrain ischemia. Neural Regen Res 11:1254–1259

51. Jung HY, Yim HS, Yoo DY et al (2016) Postnatal changes in glucose transporter 3 expression in the dentate gyrus of the C57BL/6 mouse model. Lab Anim Res 32:1–7

52. Yoo DY, Kim W, Yoo KY et al (2012) Effects of pyridoxine on a high-fat diet-induced reduction of cell proliferation and neuroblast differentiation depend on cyclic adenosine monophosphate response element binding protein in the mouse dentate gyrus. J Neurosci Res 90:1615–1625